HHS Public Access

Author manuscript

Exp Neurol. Author manuscript; available in PMC 2024 May 01.

Published in final edited form as:

Exp Neurol. 2023 May ; 363: 114358. doi:10.1016/j.expneurol.2023.114358.

UBE3A deficiency-induced autophagy is associated with activation of AMPK-ULK1 and p53 pathways

Xiaoning Hao[1], **Jiandong Sun**[1], **Li Zhong**[1], **Michel Baudry**[2], **Xiaoning Bi**[1,*]

[1]College of Osteopathic Medicine of the Pacific, Western University of Health Sciences, Pomona, CA 91766, USA,

[2]College of Dental Medicine, Western University of Health Sciences, Pomona, CA 91766, USA,

Abstract

Angelman Syndrome (AS) is a neurodevelopmental disorder caused by deficiency of the maternally expressed *UBE3A* gene. The UBE3A proteins functions both as an E3 ligase in the ubiquitin-proteasome system (UPS), and as a transcriptional co-activator for steroid hormone receptors. Here we investigated the effects of UBE3A deficiency on autophagy in the cerebellum of AS mice and in COS1 cells. Numbers and size of LC3- and LAMP2-immunopositive puncta were increased in cerebellar Purkinje cells of AS mice, as compared to wildtype mice. Western blot analysis showed an increase in the conversion of LC3I to LC3II in AS mice, as expected from increased autophagy. Levels of active AMPK and of one of its substrates, ULK1, a factor involved in autophagy initiation, were also increased. Colocalization of LC3 with LAMP2 was increased and p62 levels were decreased, indicating an increase in autophagy flux. UBE3A deficiency was also associated with reduced levels of phosphorylated p53 in the cytosol and increased levels in nuclei, which favors autophagy induction. UBE3A siRNA knockdown in COS-1 cells resulted in increased size and intensity of LC3-immunopositive puncta and increased the LC3 II/I ratio, as compared to control siRNA-treated cells, confirming the results found in the cerebellum of AS mice. These results indicate that UBE3A deficiency enhances autophagic activity through activation of the AMPK-ULK1 pathway and alterations in p53.

Keywords

Angelman syndrome; cerebellum; COS-1 cells; LC3; lysosome; mTOR; p62; siRNA; TFEB

[*]**Corresponding author:** Dr. Xiaoning Bi, Dept. of Basic Medical Sciences, COMP, Western University of Health Sciences, 701 E. Second Street, Pomona, CA 91766-1854, Tel: 909-469-5487, Fax: 909-469-5535, xbi@westernu.edu.

COI

Regarding this manuscript, the authors declare that there is no conflict of interest.

Introduction

Angelman Syndrome (AS) is a neurodevelopmental disorder with an incidence of 1 in ~15,000 live births. AS is characterized by severe developmental delay, language and cognition deficits, motor impairment (Sailer, Kaufmann et al. 2004, Berry, Leitner et al. 2005, Chamberlain, Chen et al. 2010), and in a large number of AS patients, seizure activity (Peters, Beaudet et al. 2004, Berry, Leitner et al. 2005, Dan 2009). AS is caused by the deficient expression of the maternally-inherited *UBE3A* gene in neurons (Albrecht, Sutcliffe et al. 1997, Kishino, Lalande et al. 1997, Matsuura, Sutcliffe et al. 1997, Rougeulle, Glatt et al. 1997, Vu and Hoffman 1997, Lalande and Calciano 2007, Gustin, Bichell et al. 2010). UBE3A protein has been shown to function as an E3 ligase in the ubiquitin-proteasome system (UPS) (Kishino, Lalande et al. 1997, Matsuura, Sutcliffe et al. 1997). UBE3A also functions as a co-activator and regulator of some steroid hormone receptors (Nawaz, Lonard et al. 1999, Khan, Fu et al. 2006, Catoe and Nawaz 2011), and can also affect transcription by inducing degradation of transcription factors (Nawaz, Lonard et al. 1999, Mani, Oh et al. 2006, Ramamoorthy and Nawaz 2008).

The autophagy-lysosome system is an evolutionarily conserved pathway, which degrades cellular components, e.g., misfolded or long-lived proteins and supernumerary or damaged organelles, and provides nutrients or energy in response to a variety of stresses. Autophagy plays critical roles in normal cell functions and its dysfunction has been linked to various diseases (Tooze, Dooley et al. 2015). Autophagy initiation involves the activation of Unc-51-like kinase 1 (ULK1), which recruits autophagy-relevant protein complexes, resulting in autophagy initiation in various organisms (Kim, Kundu et al. 2011; Li and Chen 2019) and in cell lines (Ryu, Kim et al. 2021). Adenosine monophosphate-activated protein kinase (AMPK) increases ULK1 activity by direct phosphorylation at several sites (Gwinn, Shackelford et al. 2008, Kim, Kundu et al. 2011, Li and Chen 2019, Van Nostrand, Hellberg et al. 2020). AMPK can also facilitate other steps in autophagy-lysosome pathways by recruiting other autophagy-relevant proteins and enhancing transcription of autophagy-related genes (Wang, Li et al. 2022). The microtubule-associated protein 1 light chain (LC3) is a mammalian homolog of autophagy-related protein 8 (Atg8) which is a ubiquitin-like protein required for the formation of autophagosomal membranes and once conjugated to phosphatidylethanolamine (PE) becomes LC3II, which is associated with autophagosomes (Tanida, Ueno et al. 2004, Liao, Yao et al. 2007, Bodemann, Orvedahl et al. 2011), and is widely used to monitor autophagy activity (Klionsky, Abdalla et al. 2012).

Perturbations in the mTOR (mechanistic target of rapamycin) pathway, which controls protein synthesis by stimulating 4EBP1 and protein degradation by inhibiting the autophagy-lysosome system, have been implicated in autism spectrum disorders (ASD) (Baron, Tepper et al. 2006, Bangash, Park et al. 2011). We previously reported that mTORC1 activity was increased while mTORC2 activity was decreased in the cerebellum of AS mice (Sun, Liu et al. 2015, Sun, Liu et al. 2018). We therefore investigated autophagic activity in the cerebellum of AS mice and COS-1 cells. As recent research, mostly in tumor cell lines, has indicated that the tumor suppressor protein, p53, regulates autophagy in a location-dependent manner with nuclear-localized p53 facilitating and cytosolic p53 suppressing autophagy (Tasdemir, Maiuri et al. 2008, Tang, Di et al. 2015, Mrakovcic and Fröhlich

2018), we also determined the potential roles of p53 in autophagy in wild-type (WT) and AS model mice.

Material and Methods

Animals

Ube3a$^{tm1Alb/J}$ mice were purchased from The Jackson Laboratory (stock No. 016590, Bar Harbor, ME), a breeding colony was established, and pup genotype was determined as previously described (Baudry, Kramar et al. 2012, Sun, Liu et al. 2015). Animal handling and experimental use followed NIH guidelines and protocols approved by the local Institutional Animal Care and Use Committee (IACUC) of Western University of Health Sciences. In all experiments male WT and AS mice aged between 2–4 months were used. Control mice were age-matched, male, WT littermates. Multiple liters were used for all experiments. Mice, housed in groups of two to three per cage, were maintained on a 12-h light/dark cycle with food and water ad libitum.

Cell culture and transfection

COS-1 cell lines were obtained from ATCC, and grown in DMEM (Dulbecco's modified Eagle's medium) supplemented with 10% (vol/vol) fetal bovine serum (FBS) at 37 °C under 5% CO_2 according to published protocols (Sun, Liu et al. 2018). To knockdown UBE3A, cells were incubated with 20 nM SMARTpool ON-TARGETplus Human UBE3A siRNA (UBE3A siRNA, GE Dharmacon, L-005137-00-0010) or ON-TARGETplus Non-targeting Control Pool (control siRNA, GE Dharmacon, D-001810-10-20) for 72 h before being used for immunofluorescence or Western blot analysis.

Immunofluorescence

For immunofluorescence with brain tissue sections, mice were sacrificed under deep anesthesia using pentobarbital administered intraperitoneally (IP) and were perfused through the left cardiac ventricle with phosphate buffered saline (PBS) followed by 4% paraformaldehyde (PFA). Whole brains were removed and post-fixed in 4% PFA overnight at 4°C followed by sequential immersion in 15% and 30% sucrose for cryoprotection. The cerebellum was then dissected and 25 μm sagittal sections were prepared with a cryomicrotome (CM 1950, LEICA). Free-floating sections were processed for immunohistochemical staining as previously described (Qin, Baudry et al. 2009, Sun, Liu et al. 2015). In brief, tissue sections were blocked for 1 h at room temperature (RT) in 5% goat serum (GS) with 0.3% Triton-X100 in 0.1 M phosphate buffer (0.3% PBST). After blocking, free-floating tissue sections were incubated in primary antibody diluted in a solution of 1% bovine serum albumin (1%BSA) with 0.3% PBST overnight at 4 °C. The following day, sections were briefly washed 3 times for 5 min each at RT in PBS followed by incubation with secondary antibodies diluted in a solution of 1% BSA with 0.3% PBST for 2 h at RT. Sections were then briefly washed 4 times for 5 min each at RT in PBS and mounted using Vectashield mounting media with DAPI (H-1200, Vector Laboratories) to stain cell nuclei. Brain sections were imaged using a Zeiss LSM 880 confocal laser-scanning microscope.

For immunofluorescence with COS-1 cells, cultured cells were fixed in 4% PFA for 15 min at 37 °C followed by 0.25% TritonX-100 in PBS for 10 min at RT. Cells were blocked with 3% BSA in PBS for 1 h at RT. After blocking, cells were incubated with primary antibody in 3% BSA/PBS overnight at 4 °C. The following day, coverslips were then washed with PBS 3 times for 5 min each at RT and then incubated with secondary antibody in 3% BSA/PBS for 2 h at RT. After washing 4 times for 5 min each with PBS, cells were mounted on glass slides using Vectashield mounting media with DAPI followed by obtaining on a Zeiss LSM 880 confocal laser-scanning microscope.

Tissue collection, P1/S1 fractionation, and Western blot analysis

Mice were deeply anesthetized with isoflurane and then decapitated. The whole brain was removed, and various brain regions (cerebellum and hippocampus) were dissected. Brain tissues were immediately used or frozen on dry ice and stored at −80 °C until further processes.

P1/S1 fractionation was prepared using the NE-PER Nuclear and Cytoplasmic Extraction Reagents Kit (Cat# 78835, Thermo Scientific) according to the manufacturer's instruction. For whole homogenates, cerebellum tissue was homogenized in RIPA buffer (10 mM Tris, pH 8, 140 mM NaCl, 1 mM EDTA, 0.5 mM EGTA, 1% NP-40, 0.5% sodium deoxycholate, and 0.1% SDS and a protease inhibitor cocktail). Cultured COS-1 cells were lysed in lysis buffer (Tris-HCl 25 mM pH 7.4, NaCl 150 mM, 1 mM EDTA, 5% glycerol, 0.5% CHAPS and a protease inhibitor cocktail). The total protein concentration of the resultant samples was measured with a BCA protein assay kit (Pierce, Prod# 23225, Thermo fisher Scientific).

Western blot were performed using previously published protocols (Sun, Zhu et al. 2015). In brief, proteins were separated by SDS-PAGE followed by transfer to PVDF membranes (Cat# IPFL00010, Millipore). After incubation with 3% BSA/TBS (Tris-buffered saline) at RT for 1 h, membranes were incubated with specific primary antibodies overnight at 4 °C. Following incubation in primary antibodies, membranes were washed with TBST (Tris-buffered saline with Tween-20) three times; 5 min each wash, at RT, and then incubated with secondary antibodies (IRDye secondary antibodies) for 2 h at RT with gentle shaking. The specific protein bands were analyzed with the Odyssey imaging system and LI-COR Image Studio Software.

Antibodies

The following antibodies were used: LC3-B-N-Terminus (1:200, catalog#0231–100/ LC3–5F10, Nanotools); LC3-B-N-Terminus (1:500, catalog#AP1802a, Abgent); Anti-LC3 mAb (1:50, catalog#M152–3, MBL); LAMP2 (1:200; catalog#ab13524; Abcam); UBE3A (1:1000, catalog#A300–351A, Bethyl); GAPDH (1:1000, catalog#MAB374, EMD Millipore); LaminB1 (1:1000, catalog#ab16048, Abcam); p62/SQSTM1 (1:1000, catalog#16-RB62, American Research Products); AMPK (1:1000, catalog#2532S, Cell Signaling Technology); AMPK-Thr172 (1:1000, catalog#2535S, Cell Signaling Technology); ULK1-Ser757 (1:1000, catalog#6888, Cell Signaling Technology); ULK1 (1:500, catalog#ab65056, Abcam); ULK1-Ser777 (1:1000, catalog#ABC213, Sigma); ULK1-Ser317 (1:1000, catalog#37762S, Cell Signaling Technology); 4EBP1-Ser65

(1:1000, catalog#9451, Cell Signaling Technology); 4EBP1 (1:1000, catalog#9644S, Cell Signaling Technology); Cathepsin B (1:500, catalog#AF965, R&D System); p53 (1:200, catalog#AHO0112, Invitrogen); p53-Ser15 (1:1000, catalog#9286L, Cell Signaling Technology); p53-Ser15 (1:1000, catalog#9284L, Cell Signaling Technology); Calbindin (1:500, catalog#300, Swant); TFEB (1:1000, catalog#A303–673A, Bethyl); Goat anti-rabbit IgG IRDye® 680RD (1:10000, catalog#926–68071, LI-COR Biosciences); Goat anti-mouse IgG IRDye® 800CW (1:10000, catalog#926–32210, LI-COR Biosciences); Donkey anti-goat IgG IRDye® 800CW (1:10000, catalog#926–32214, LI-COR Biosciences); Goat anti-rabbit IgG AlexaFluor 594 (1:200, catalog#A-11037, Invitrogen); Goat anti-mouse IgG AlexaFluor 594 (1:200, catalog#A-11005, Invitrogen); Goat anti-rat IgG AlexaFluor 488 (1:400, catalog#A-11006, Invitrogen); Goat anti-rabbit IgG AlexaFluor 488 (1:400, catalog#A-11008, Invitrogen); Goat anti-mouse IgG AlexaFluor 488 (1:400, catalog# A-11029, Invitrogen).

Image analysis, quantification, and statistical analysis

Slides were imaged by using a Zeiss LSM 880 confocal microscope and pictures were analyzed with the particle analysis macro of NIH ImageJ. After splitting channels, images from different experimental groups were first thresholded at the same level, individual cells were then outlined, and 20–30 cells per brain were analyzed. The colocalization coefficient was analyzed using Zeiss ZEN Microscopy Software. Results are presented as means ± SEM. To determine p values, the unpaired Student's t test was used, as indicated in the figure legends. Results with a p value <0.05 were considered statistically significant.

Results

1. Increased activation of the autophagy-lysosome system in cerebellum of AS mice

Immunofluorescence staining showed that UBE3A expression was prominent in cell bodies and dendrites of Purkinje neurons in WT mice and was markedly reduced in AS mice (Fig. 1A). To determine autophagic-lysosome activity, we analyzed levels and co-localization of LC3 and LAMP2, a protein associated with lysosomal membranes and required for lysosomal fusion with autophagosomes (Huynh, Eskelinen et al. 2007). LC3- and LAMP2-immunoreactivity (ir) was present in both puncta and diffused form in cell bodies of Purkinje cell neurons from AS and WT mice (Fig. 1B). Quantitative analysis of LC3- and LAMP2-ir in Purkinje neurons revealed a significant increase in the number and size of LC3- and LAMP2-positive puncta in AS mice, as compared to WT mice (Fig. 1C, D). The intensity of LC3- and LAMP2-ir was also increased in AS mice, however, this did not reach statistical significance. These results suggest an increased autophagy initiation and flux. LC3-ir was partially co-localized with LAMP2-ir in both WT and AS mice. Image analysis indicated that the number of puncta stained with both LC3 and LAMP2 antibodies was significantly increased in AS mice (Fig. 1E). Western blot analysis of cerebellar homogenates indicated that the ratio of LC3II/LC3I was significantly increased in the cerebellum of AS mice, as compared to WT mice (Fig. 1F, G). The ratio LC3II/LC3I was also increased in the hippocampus of AS mice (Supplement Fig. 1A).

2. Changes in autophagy-related proteins in nuclear and cytoplasmic fractions in the cerebellum of AS mice

LC3 is localized in the cytosol and enriched in nucleoli where it is conjugated with high-molecular weight complexes (Kraft, Manral et al. 2016). Accumulating evidence suggests that nuclear LC3 and its translocation to the cytoplasm play critical roles in autophagy initiation and cell survival (Huang, Xu et al. 2015, Papandreou and Tavernarakis 2019). We analyzed LC3 and other autophagy-related proteins in cerebellar nuclear (P1) and cytoplasmic (S1) fractions from WT and AS mice. LC3II/I ratio was increased in both P1 and S1 fractions from AS mice, as compared to WT mice (Fig. 2A–C). We also analyzed the levels of p62 (also known as SQSTM1) in both P1 and S1 fractions. P62 is a receptor for ubiquitinated proteins and other cargos destined for lysosomal degradation (Cohen-Kaplan, Livneh et al. 2016), and its level is generally inversely correlated with autophagic activity and flux (Rogov, Dötsch et al. 2014). P62 levels were significantly reduced in S1 fractions from AS mice (Fig. 2A, B), but there was no significant difference in P1 fractions between WT and AS mice (Supplement Fig. 1C). To further confirm that increased LC3II levels were not due to decreased lysosomal function, we determined levels of cathepsin B, a lysosomal protease that is expressed mainly in late endosomal/lysosomal compartments. No significant changes were observed for levels of cathepsin B (Fig. 2A and Supplement Fig. 1C). These results suggest that autophagic initiation and flux, indicated by increased LC3II and decreased p62 levels respectively, are elevated in the cerebellum of AS mice.

We previously reported that mTORC1 activity was increased in AS mice (Sun, Liu et al. 2015), which raises the question of how could both mTOR activation and autophagy be increased in AS mice, since they exhibit a mutual inhibitory relationship. AMPK, a heterotrimeric protein responsible for the detection of energy levels, has been shown to regulate both mTORC1 and autophagy. Activation of AMPK inhibits mTORC1 signaling but promotes autophagy initiation and flux by phosphorylating ULK1 and other autophagy-related proteins (Gwinn, Shackelford et al. 2008, Kim, Kundu et al. 2011, Li and Chen 2019, Van Nostrand, Hellberg et al. 2020). We analyzed the levels of total AMPK and of its active form p-Thr172-AMPK by Western blot. The ratio AMPK-Thr172/AMPK was markedly elevated in S1 fractions in AS mice, as compared to WT mice (Fig. 2A, B), while it was no changed in P1 fraction (Supplement Fig. 1C). These results suggest that active cytosolic AMPK could be responsible for increased autophagy in AS mice. We next evaluated the levels of total ULK1, ULK1-Ser757 (phosphorylated by mTORC1 and a negative regulator of autophagy initiation), and ULK1-Ser777 and ULK1-Ser317 (phosphorylated by AMPK and a positive regulators of autophagy initiation). Levels of total ULK1 were significantly increased in P1 fractions from the cerebellum of AS mice as compared to WT mice (Fig. 2A, C); a similar effect was also observed in S1 fractions, but this was not statistically significant (Supplement Fig. 1C). The various phosphorylated forms of ULK1 (ULK1-Ser317, ULK1-Ser757, and ULK1-Ser777) were mostly observed in S1 fractions (Fig. 2A and Supplement Fig. 1B, C), and only the ratio ULK1-Ser317/ULK1 was significantly increased in S1 fractions of AS mice, as compared to WT mice (Fig. 2A, B), suggesting that ULK1 activation by AMPK plays a dominant role in AS mice.

To evaluate mTORC1 activity, we measured the levels of the eukaryotic translation initiation factor 4E (eIF4E)-binding protein 1 (4EBP1) and of 4EBP1-Ser65 (phosphorylated by mTORC1) (Qin, Jiang et al. 2016, Woodcock, Eley et al. 2019). Total 4EBP1 was mostly found in S1 fractions and its level was significantly reduced in AS mice (Fig. 2A, B); a very lightly-labeled band was observed in P1 with enhanced exposure (not shown). In contrast, 4EBP1-Ser65 was mainly found in P1 fractions and its level was increased in AS mice (Fig. 2A, C). Immunofluorescent labeling of 4EBP1-Ser65 further confirmed these results; 4EBP1-Ser65-ir was mostly present in nuclei and staining intensity was increased in AS mice (Supplement Fig. 2A). Recent studies have shown that 4EBP1 translocates from the cytoplasm to the nucleus where it may regulate transcription (Takahashi, Shibutani et al. 2022). How 4EBP1-Ser65 nuclear translocation is regulated and whether this plays an important role in AS pathogenesis remains to be determined.

mTORC1 also phosphorylates TFEB and prevents its nuclear translocation to regulate lysosomal and autophagic function (Napolitano, Esposito et al. 2018, Puertollano, Ferguson et al. 2018). We examined total TFEB and its phosphorylated forms at Ser142 and Ser211. Levels of total TFEB in P1 fractions were not different between WT and AS mice (Fig. 2A, C), but TFEB levels were significantly lower in S1 fractions from AS mice, as compared to WT mice (Fig. 2A, B). Levels of TFEB phosphorylated at Ser142 and Ser211 were not significantly different between AS and WT mice in both S1 and P1 fractions (not shown). These results suggest that increased autophagy in the cerebellum of AS mice is most likely caused by increased AMPK activation followed by ULK1 activation and possibly nuclear translocation of TFEB as well.

3. Changes in phosphorylated p53 (p53-Ser15) in cerebellum of AS mice

Accumulating evidence indicates that the tumor suppressor p53 plays important roles in autophagy regulation, as it functions both as an autophagy inducer, when it is located in the nuclei, and an autophagy suppressor, when it is located in the cytosol (Tasdemir, Maiuri et al. 2008, Tang, Di et al. 2015, Mrakovcic and Fröhlich 2018). Western blot analysis of P1 and S1 fractions from the cerebellum showed that the ratio p53-Ser15/p53 was reduced in S1 fractions of AS mice as compared to WT mice, while it was increased in P1 fractions from AS mice, although this did not reach statistical significance (Fig. 3A, B). Immunofluorescent staining showed prominent p53-Ser15-ir within the cell bodies and dendrites of Purkinje cell layer (Supplement Fig. 2B), which was partially co-localized with LC3 staining, and more p53-Ser15/LC3 double-stained puncta were detected in AS than in WT mice (Fig. 3C, D).

4. UBE3A knock-down in COS1 cells increased LC3-ir puncta size and intensity, LC3II/LC3I ratio, and p53 phosphorylation

To further characterize the role of UBE3A in autophagy, we carried out in vitro experiments in COS-1 cells and used siRNA knockdown of UBE3A. A significant decrease in the intensity of UBE3A-ir was observed in cells treated with UBE3A siRNA as compared with cells treated with a scrambled siRNA (control siRNA) (Fig. 4A,D). The knockdown effects was confirmed by Western blot analysis (Fig.4C,D). The effects of UBE3A knockdown on LC3 expression were determined by both immunofluorescent staining and Western blot analysis (Fig. 4). While many LC3-ir puncta were observed in scrambled siRNA- (control

siRNA) treated cells, LC3-ir puncta in UBE3A siRNA-treated cells were larger and the staining brighter (Fig. 4A). These observations were confirmed by image quantification (Fig. 4B). We next determined the ratio of LC3II to LC3I and the levels of p62 in whole homogenates from both control siRNA- and UBE3A siRNA-treated COS-1 cells. Like in the cerebellum of AS mice, UBE3A knockdown increased the ratio LC3II/I and reduced the levels of p62 (Fig. 4C, D). Subcellular fractionation results showed that the ratio LC3 II/I was significantly increased in both P1 and S1 fractions (Fig. 4E, F). Western blot analysis showed that p53-Ser15 was present predominantly in P1 fractions from COS-1 cells, which is different from our in vivo experiments. The difference could be due to the different types of cells; p53-Ser15 mainly functions in the nuclei of tumorous cells, while in the cerebellum it is mostly localized in the cytosol. Levels of p53-Ser15 were significantly increased in P1 fractions following UBE3A knockdown in COS-1 cells (Fig. 4E, F). These results indicate that UBE3A deficiency increases autophagy in COS-1 cells as it does in mouse cerebellum.

Discussion

In the present study, we found that UBE3A deficiency increased the ratio LC3II/LC3I in AS cerebellum, indicating increased LC3I to LC3II conversion and autophagy induction. We also found that the colocalization of LC3 with LAMP2 was increased while p62 levels were decreased in AS cerebellum, indicating that the autophagy flux was increased. We further showed that UBE3A knockdown in COS-1 cells resulted in similar changes, namely increased LC3II/LC3I ratio and decreased p62 levels. Together, these results indicate that UBE3A deficiency increases autophagy activity. These results are consistent with a recent report showing that UBE3A deficiency results in increased autophagy in primary cortical neurons of AS mice (Wang, Wang et al. 2019). Mechanistically, we found that the active forms of both AMPK and ULK1 were upregulated in the cerebellum of AS mice as compared to WT mice, suggesting that activation of AMPK and of its downstream substrate ULK1 may be important for increased autophagic activity. AMPK has multiple downstream targets, which are critical for maintaining cellular energy homeostasis, and some of them are directly or indirectly linked to autophagy regulation at multiple levels. In particular, AMPK phosphorylates ULK1 at Ser317 and Ser777 to promote autophagy induction (Kim, Kundu et al. 2011); ULK1 functions as an essential initiator for autophagy (Zachari and Ganley 2017, Torii, Yamaguchi et al. 2020). AMPK can also increase the function of class III PI3K to promote autophagy initiation (Kahn, Alquier et al. 2005). Finally, AMPK promotes autophagy initiation by inhibiting mTORC1 activity since it phosphorylates TSC2 at Ser1387 and Raptor at Ser792, thereby inhibiting mTORC1 signaling pathway (Gwinn, Shackelford et al. 2008, Van Nostrand, Hellberg et al. 2020). mTORC1 phosphorylates ULK1 at Ser757 and disrupts ULK1-AMPK interactions, thereby suppressing autophagy induction (Kim, Kundu et al. 2011, Nakatogawa 2020). Our results showed that while AMPK-mediated phosphorylation of ULK1 was increased, that by mTORC1 was not, indicating that in AS mice AMPK-mediated regulation of ULK1 is dominant. AMPK has also been associated with autophagosome biogenesis, maturation, and fusion with lysosomes to promote autophagy flux (Dunlop and Tee 2013, Jang, Park et al. 2018). Additionally, AMPK promotes TFEB-mediated upregulation of autophagy-relevant genes through SIRT1 activation (Huang, Wang et al. 2019, Liu, Liu et al. 2021). TFEB is dephosphorylated

when mTORC1 is inactive, which leads to the separation of TFEB from 14-3-3, followed by TFEB nuclear translocation and the initiation of transcriptional regulation of lysosomal biogenesis and autophagy. However, TFEB activation (TFEB dephosphorylation) has also been reported despite high mTORC1 activity, such as under ER stress, pathogen infection, and oxidative stress (Roczniak-Ferguson, Petit et al. 2012, Puertollano, Ferguson et al. 2018). In our study, we found that total TFEB levels decreased in S1 fractions with no change in P1 fractions from AS mice, as compared to WT mice, which suggests that TFEB nuclear translocation might regulate the expression of autophagy-related proteins in AS mice. These results indicate that, although mTORC1 activity is high, it may not reach the levels required to block TFEB nuclear translocation in the cerebellum of AS mice, due to enhanced AMPK activity. Alternatively, enhanced dephosphorylation by various phosphatases, such as calcineurin, may contribute to TFEB translocation in AS mice. Thus, activation of AMPK-ULK1 pathway could facilitate autophagy initiation and completion, despite enhanced mTORC1 activation in AS cerebellum (Sun, Liu et al. 2015).

Another pathway that may contribute to enhanced autophagy in AS mice is the p53 pathway. Recent evidence has demonstrated that p53 is involved in regulating autophagic activity both positively and negatively. As a transcription factor, p53 activates pro-autophagic genes in the nucleus, while cytoplasmic p53 enhances cell death and blocks autophagy (Feng, Zhang et al. 2005, Tasdemir, Maiuri et al. 2008, Mrakovcic and Fröhlich 2018). We showed that UBE3A knockdown significantly increased p53-Ser15 in P1 fractions in COS-1 cells and that UBE3A deficiency resulted in decreased p53-Ser15 in S1 fractions in AS mice; both changes favor autophagy induction. These results are consistent with the recent report that p53-Ser15 could activate autophagy in the nucleus and block autophagy in the cytoplasm (Mrakovcic and Fröhlich 2018). Further studies are needed to investigate whether p53-Ser15 depletion and inhibition could affect autophagy in both cell lines and in AS mice. Functionally, the enhanced autophagy activity may compensate for reduced UPS function in AS mice.

Autophagy and UPS are two pivotal intracellular degradation pathways controling protein quality and maintaining cellular metabolism and homeostasis. Recent studies have revealed dynamic interconnections and metabolic compensation between these two systems (Kocaturk and Gozuacik 2018, Zientara-Rytter and Subramani 2019), and accumulating evidence shows that the autophagy-lysosome system is also activated by misfolded proteins and aggregation-induced ER stress, although these processes generally first activate the UPS. Dysfunction of the UPS pathway is closely associated with enhanced autophagy as emerging evidence indicates that depletion of E3 ubiquitin ligases impairs protein ubiquitination and degradation and induces autophagy (Wang, Xia et al. 2018, Che, Yang et al. 2019, Lee, Yoo et al. 2020, Yang, Zhu et al. 2022). A selective autophagy pathway, referred to as aggrephagy, has been intensively investigated in a number of neurodegenerative disorders associated with protein misfolding and aggregation, such as tauopathies, synucleinopathies, and polyglutamine-containing inclusions or TAR DNA binding protein-43 (TDP-43) proteinopathies (Jimenez-Sanchez, Thomson et al. 2012, Fox 2016). In this process, misfolded proteins are ubiquitinated and aggregated with p62, which together with NBR1, functions as cargo receptors for autophagy (Lamark, Kirkin et al. 2009). Two recent studies have indicated that UBE3A may participate in protein folding

quality control. In particular, UBE3A interacts with the chaperone protein HSP70 and promotes the degradation of HSP70-bound substrates (Mishra, Godavarthi et al. 2009). Thus, the lack of functional UBE3A could result in accumulation of misfolded proteins and activation of the autophagy-lysosome system. In addition, sacsin, the protein involved in spastic ataxia of Charlevoix-Saguenay, is a potential UBE3A substrate, exhibits an HSP90 homology domain, and promotes protein folding (Anderson, Siller et al. 2011). If sacsin were to be confirmed as a UBE3A substrate, then the lack of UBE3A would lead to sacsin accumulation, which could result in improved protein folding. Whether UBE3A directly or indirectly participates in protein quality control remains therefore an interesting question.

Conclusions

In our study, we showed that UBE3A deficiency enhances autophagy induction and completion mainly by activation of the AMPK-ULK1 pathway. TFEB-induced transcriptional regulation may also contribute to enhanced autophagy activity, as well as enhanced nuclear and reduced cytosol p53 activation. Finally, AMPK may also suppress mTORC1 activation, which in turn stimulates autophagy. Whether enhanced autophagy is a compensatory mechanism to sustain metabolic homeostasis or a pathogenic process for Angelman Syndrome remain to be determined. Additionally, as both UPS and autophagy have been implicated in various diseases, our results, which provide further evidence for the mutual regulation of these two systems, may have broad implications.

Supplementary Material

Refer to Web version on PubMed Central for supplementary material.

Acknowledgments

This work was supported by grants R01NS104078 from NIH/NINDS to MB and R15MH101703 from NIH/NIMH to XB. XB is also supported by funds from the Daljit and Elaine Sarkaria Chair.

References

Albrecht U, Sutcliffe JS, Cattanach BM, Beechey CV, Armstrong D, Eichele G and Beaudet AL (1997). “Imprinted expression of the murine Angelman syndrome gene, Ube3a, in hippocampal and Purkinje neurons.” Nat Genet 17(1): 75–78. DOI: 10.1038/ng0997-75 [PubMed: 9288101]

Anderson JF, Siller E and Barral JM (2011). “The neurodegenerative-disease-related protein sacsin is a molecular chaperone.” J Mol Biol 411(4): 870–880. DOI: 10.1016/j.jmb.2011.06.016 [PubMed: 21726565]

Bangash MA, Park JM, Melnikova T, Wang D, Jeon SK, Lee D, Syeda S, Kim J, Kouser M and Schwartz J (2011). RETRACTED: Enhanced polyubiquitination of shank3 and NMDA receptor in a mouse model of Autism, Elsevier. DOI: 10.1016/j.cell.2011.03.052

Baron CA, Tepper CG, Liu SY, Davis RR, Wang NJ, Schanen NC and Gregg JP (2006). “Genomic and functional profiling of duplicated chromosome 15 cell lines reveal regulatory alterations in UBE3A-associated ubiquitin–proteasome pathway processes.” Human molecular genetics 15(6): 853–869. DOI: 10.1093/hmg/ddl004 [PubMed: 16446308]

Baudry M, Kramar E, Xu X, Zadran H, Moreno S, Lynch G, Gall C and Bi X (2012). “Ampakines promote spine actin polymerization, long-term potentiation, and learning in a mouse model of Angelman syndrome.” Neurobiology of disease 47(2): 210–215. DOI: 10.1016/j.nbd.2012.04.002 [PubMed: 22525571]

Berry RJ, Leitner RP, Clarke AR and Einfeld SL (2005). "Behavioral aspects of Angelman syndrome: A case control study." American Journal of Medical Genetics Part A 132(1): 8–12. DOI: 10.1002/ajmg.a.30154

Bodemann BO, Orvedahl A, Cheng T, Ram RR, Ou Y-H, Formstecher E, Maiti M, Hazelett CC, Wauson EM and Balakireva M (2011). "RalB and the exocyst mediate the cellular starvation response by direct activation of autophagosome assembly." Cell 144(2): 253–267. DOI: 10.1016/j.cell.2010.12.018 [PubMed: 21241894]

Catoe HW and Nawaz Z (2011). "E6-AP facilitates efficient transcription at estrogen responsive promoters through recruitment of chromatin modifiers." Steroids 76(9): 897–902. DOI: 10.1016/j.steroids.2011.04.007 [PubMed: 21530567]

Chamberlain SJ, Chen P-F, Ng KY, Bourgois-Rocha F, Lemtiri-Chlieh F, Levine ES and Lalande M (2010). "Induced pluripotent stem cell models of the genomic imprinting disorders Angelman and Prader–Willi syndromes." Proceedings of the National Academy of Sciences 107(41): 17668–17673. DOI: 10.1073/pnas.1004487107

Che L, Yang X, Ge C, El-Amouri SS, Wang Q-E, Pan D, Herzog TJ and Du C (2019). "Loss of BRUCE reduces cellular energy level and induces autophagy by driving activation of the AMPK-ULK1 autophagic initiating axis." PLoS One 14(5): e0216553. DOI: 10.1371/journal.pone.0216553 [PubMed: 31091257]

Cohen-Kaplan V, Livneh I, Avni N, Fabre B, Ziv T, Kwon YT and Ciechanover A (2016). "p62-and ubiquitin-dependent stress-induced autophagy of the mammalian 26S proteasome." Proceedings of the National Academy of Sciences 113(47): E7490–E7499. DOI: 10.1073/pnas.1615455113

Dan B (2009). "Angelman syndrome: current understanding and research prospects." Epilepsia 50(11): 2331–2339. DOI: 10.1111/j.1528-1167.2009.02311.x [PubMed: 19874386]

Dunlop EA and Tee AR (2013). "The kinase triad, AMPK, mTORC1 and ULK1, maintains energy and nutrient homoeostasis." Biochemical Society Transactions 41(4): 939–943. DOI: 10.1042/BST20130030 [PubMed: 23863160]

Feng Z, Zhang H, Levine AJ and Jin S (2005). "The coordinate regulation of the p53 and mTOR pathways in cells." Proceedings of the National Academy of Sciences 102(23): 8204–8209. DOI: 10.1073/pnas.0502857102

Gustin RM, Bichell TJ, Bubser M, Daily J, Filonova I, Mrelashvili D, Deutch AY, Colbran RJ, Weeber EJ and Haas KF (2010). "Tissue-specific variation of Ube3a protein expression in rodents and in a mouse model of Angelman syndrome." Neurobiol Dis 39(3): 283–291. DOI: 10.1016/j.nbd.2010.04.012 [PubMed: 20423730]

Gwinn DM, Shackelford DB, Egan DF, Mihaylova MM, Mery A, Vasquez DS, Turk BE and Shaw RJ (2008). "AMPK phosphorylation of raptor mediates a metabolic checkpoint." Molecular cell 30(2): 214–226. DOI: 10.1016/j.molcel.2008.03.003 [PubMed: 18439900]

Huang J, Wang X, Zhu Y, Li Z, Zhu YT, Wu JC, Qin ZH, Xiang M and Lin F (2019). "Exercise activates lysosomal function in the brain through AMPK-SIRT1-TFEB pathway." CNS neuroscience & therapeutics 25(6): 796–807. DOI: 10.1111/cns.13114 [PubMed: 30864262]

Huang R, Xu Y, Wan W, Shou X, Qian J, You Z, Liu B, Chang C, Zhou T and Lippincott-Schwartz J (2015). "Deacetylation of nuclear LC3 drives autophagy initiation under starvation." Molecular cell 57(3): 456–466. DOI: 10.1016/j.molcel.2014.12.013 [PubMed: 25601754]

Huynh KK, Eskelinen EL, Scott CC, Malevanets A, Saftig P and Grinstein S (2007). "LAMP proteins are required for fusion of lysosomes with phagosomes." The EMBO journal 26(2): 313–324. DOI: 10.1038/sj.emboj.7601511 [PubMed: 17245426]

Jang M, Park R, Kim H, Namkoong S, Jo D, Huh YH, Jang I-S, Lee JI and Park J (2018). "AMPK contributes to autophagosome maturation and lysosomal fusion." Scientific reports 8(1): 1–10. DOI: 10.1038/s41598-018-30977-7 [PubMed: 29311619]

Jimenez-Sanchez M, Thomson F, Zavodszky E and Rubinsztein DC (2012). "Autophagy and polyglutamine diseases." Progress in Neurobiology 97(2): 67–82. DOI: 10.1016/j.pneurobio.2011.08.013 [PubMed: 21930185]

Kahn BB, Alquier T, Carling D and Hardie DG (2005). "AMP-activated protein kinase: ancient energy gauge provides clues to modern understanding of metabolism." Cell metabolism 1(1): 15–25. DOI: 10.1016/j.cmet.2004.12.003 [PubMed: 16054041]

Khan OY, Fu G, Ismail A, Srinivasan S, Cao X, Tu Y, Lu S and Nawaz Z (2006). “Multifunction steroid receptor coactivator, E6-associated protein, is involved in development of the prostate gland.” Molecular endocrinology 20(3): 544–559. DOI: 10.1210/me.2005-0110 [PubMed: 16254014]

Kim J, Kundu M, Viollet B and Guan K-L (2011). “AMPK and mTOR regulate autophagy through direct phosphorylation of Ulk1.” Nature cell biology 13(2): 132–141. DOI: 10.1038/ncb2152 [PubMed: 21258367]

Kishino T, Lalande M and Wagstaff J (1997). “UBE3A/E6-AP mutations cause Angelman syndrome.” Nat Genet 15(1): 70–73. DOI: 10.1038/ng0197-70 [PubMed: 8988171]

Klionsky DJ, Abdalla FC, Abeliovich H, Abraham RT, Acevedo-Arozena A, Adeli K, Agholme L, Agnello M, Agostinis P and Aguirre-Ghiso JA (2012). “Guidelines for the use and interpretation of assays for monitoring autophagy.” Autophagy 8(4): 445–544. DOI: 10.4161/auto.19496 [PubMed: 22966490]

Kocaturk NM and Gozuacik D (2018). “Crosstalk between mammalian autophagy and the ubiquitin-proteasome system.” Frontiers in cell and developmental biology: 128. DOI: 10.3389/fcell.2018.00128 [PubMed: 30333975]

Kraft LJ, Manral P, Dowler J and Kenworthy AK (2016). “Nuclear LC3 associates with slowly diffusing complexes that survey the nucleolus.” Traffic 17(4): 369–399. DOI: 10.1111/tra.12372 [PubMed: 26728248]

Lalande M and Calciano MA (2007). “Molecular epigenetics of Angelman syndrome.” Cell Mol Life Sci 64(7–8): 947–960. DOI: 10.1007/s00018-007-6460-0 [PubMed: 17347796]

Lamark T, Kirkin V, Dikic I and Johansen T (2009). “NBR1 and p62 as cargo receptors for selective autophagy of ubiquitinated targets.” Cell Cycle 8(13): 1986–1990. DOI: 10.4161/cc.8.13.8892 [PubMed: 19502794]

Lee D-E, Yoo JE, Kim J, Kim S, Kim S, Lee H and Cheong H (2020). “NEDD4L downregulates autophagy and cell growth by modulating ULK1 and a glutamine transporter.” Cell death & disease 11(1): 1–17. DOI: 10.1038/s41419-020-2242-5 [PubMed: 31911576]

Li Y and Chen Y (2019). “AMPK and Autophagy.” Adv Exp Med Biol 1206: 85–108. DOI: 10.1007/978-981-15-0602-4_4 [PubMed: 31776981]

Liao G, Yao Y, Liu J, Yu Z, Cheung S, Xie A, Liang X and Bi X (2007). “Cholesterol accumulation is associated with lysosomal dysfunction and autophagic stress in Npc1−/− mouse brain.” The American journal of pathology 171(3): 962–975. DOI: 10.2353/ajpath.2007.070052 [PubMed: 17631520]

Liu L, Liu C and Fang L (2021). “AMPK-SIRT1 pathway dysfunction contributes to neuron apoptosis and cognitive impairment induced by sevoflurane.” Molecular Medicine Reports 23(1): 1–1. DOI: 10.3892/mmr.2020.11694

Mani A, Oh AS, Bowden ET, Lahusen T, Lorick KL, Weissman AM, Schlegel R, Wellstein A and Riegel AT (2006). “E6AP mediates regulated proteasomal degradation of the nuclear receptor coactivator amplified in breast cancer 1 in immortalized cells.” Cancer research 66(17): 8680–8686. DOI: 10.1158/0008-5472.CAN-06-0557 [PubMed: 16951183]

Matsuura T, Sutcliffe JS, Fang P, Galjaard R-J, Jiang Y.-h., Benton CS, Rommens JM and Beaudet AL (1997). “De novo truncating mutations in E6-AP ubiquitin-protein ligase gene (UBE3A) in Angelman syndrome.” Nature genetics 15(1): 74–77. DOI: 10.1038/ng0197-74 [PubMed: 8988172]

Mishra A, Godavarthi SK, Maheshwari M, Goswami A and Jana NR (2009). “The ubiquitin ligase E6-AP is induced and recruited to aggresomes in response to proteasome inhibition and may be involved in the ubiquitination of Hsp70-bound misfolded proteins.” Journal of biological chemistry 284(16): 10537–10545. DOI: 10.1074/jbc.M806804200 [PubMed: 19233847]

Mrakovcic M and Fröhlich LF (2018). “p53-mediated molecular control of autophagy in tumor cells.” Biomolecules 8(2): 14. DOI: 10.3390/biom8020014 [PubMed: 29561758]

Nakatogawa H (2020). “Mechanisms governing autophagosome biogenesis.” Nature reviews Molecular cell biology 21(8): 439–458. DOI: 10.1038/s41580-020-0241-0 [PubMed: 32372019]

Napolitano G, Esposito A, Choi H, Matarese M, Benedetti V, Di Malta C, Monfregola J, Medina DL, Lippincott-Schwartz J and Ballabio A (2018). “mTOR-dependent phosphorylation controls TFEB nuclear export.” Nature communications 9(1): 1–10. DOI: 10.1038/s41467-018-05862-6

Nawaz Z, Lonard DM, Dennis AP, Smith CL and O’Malley BW (1999). “Proteasome-dependent degradation of the human estrogen receptor.” Proceedings of the National Academy of Sciences 96(5): 1858–1862. DOI: 10.1073/pnas.96.5.1858

Nawaz Z, Lonard DM, Smith CL, Lev-Lehman E, Tsai SY, Tsai M-J and O’Malley BW (1999). “The Angelman syndrome-associated protein, E6-AP, is a coactivator for the nuclear hormone receptor superfamily.” Molecular and cellular biology 19(2): 1182–1189. DOI: 10.1128/MCB.19.2.1182 [PubMed: 9891052]

Papandreou M-E and Tavernarakis N (2019). “Nucleophagy: from homeostasis to disease.” Cell Death & Differentiation 26(4): 630–639. DOI: 10.1038/s41418-018-0266-5 [PubMed: 30647432]

Peters S, Beaudet A, Madduri N and Bacino C (2004). “Autism in Angelman syndrome: implications for autism research.” Clinical genetics 66(6): 530–536. DOI: 10.1111/j.1399-0004.2004.00362.x [PubMed: 15521981]

Puertollano R, Ferguson SM, Brugarolas J and Ballabio A (2018). “The complex relationship between TFEB transcription factor phosphorylation and subcellular localization.” The EMBO journal 37(11): e98804. DOI: 10.15252/embj.201798804 [PubMed: 29764979]

Qin Q, Baudry M, Liao G, Noniyev A, Galeano J and Bi X (2009). “A novel function for p53: regulation of growth cone motility through interaction with Rho kinase.” Journal of Neuroscience 29(16): 5183–5192. DOI: 10.1523/JNEUROSCI.0420-09.2009 [PubMed: 19386914]

Qin X, Jiang B and Zhang Y (2016). “4E-BP1, a multifactor regulated multifunctional protein.” Cell cycle 15(6): 781–786. DOI: 10.1080/15384101.2016.1151581 [PubMed: 26901143]

Ramamoorthy S and Nawaz Z (2008). “E6-associated protein (E6-AP) is a dual function coactivator of steroid hormone receptors.” Nuclear receptor signaling 6. DOI: 10.1621/nrs.06006

Roczniak-Ferguson A, Petit CS, Froehlich F, Qian S, Ky J, Angarola B, Walther TC and Ferguson SM (2012). “The transcription factor TFEB links mTORC1 signaling to transcriptional control of lysosome homeostasis.” Science signaling 5(228): ra42–ra42. DOI: 10.1126/scisignal.2002790 [PubMed: 22692423]

Rogov V, Dötsch V, Johansen T and Kirkin V (2014). “Interactions between autophagy receptors and ubiquitin-like proteins form the molecular basis for selective autophagy.” Molecular cell 53(2): 167–178. DOI: 10.1016/j.molcel.2013.12.014 [PubMed: 24462201]

Rougeulle C, Glatt H and Lalande M (1997). “The Angelman syndrome candidate gene, UBE3A/E6-AP, is imprinted in brain.” Nat Genet 17(1): 14–15. DOI: 10.1038/ng0997-14 [PubMed: 9288088]

Ryu HY, Kim LE, Jeong H, Yeo BK, Lee J-W, Nam H, Ha S, An H-K, Park H and Jung S (2021). “GSK3B induces autophagy by phosphorylating ULK1.” Experimental & molecular medicine 53(3): 369–383. DOI: 10.1038/s12276-021-00570-6 [PubMed: 33654220]

Sun J, Liu Y, Jia Y, Hao X, ju Lin W, Tran J, Lynch G, Baudry M and Bi X (2018). “UBE3A-mediated p18/LAMTOR1 ubiquitination and degradation regulate mTORC1 activity and synaptic plasticity.” Elife 7: e37993. DOI: 10.7554/eLife.37993 [PubMed: 30020076]

Sun J, Liu Y, Moreno S, Baudry M and Bi X (2015). “Imbalanced mechanistic target of rapamycin C1 and C2 activity in the cerebellum of Angelman syndrome mice impairs motor function.” Journal of Neuroscience 35(11): 4706–4718. DOI: 10.1523/JNEUROSCI.4276-14.2015 [PubMed: 25788687]

Sun J, Zhu G, Liu Y, Standley S, Ji A, Tunuguntla R, Wang Y, Claus C, Luo Y and Baudry M (2015). “UBE3A regulates synaptic plasticity and learning and memory by controlling SK2 channel endocytosis.” Cell reports 12(3): 449–461. DOI: 10.1016/j.celrep.2015.06.023 [PubMed: 26166566]

Takahashi S, Shibutani S and Iwata H (2022). “Nuclear-targeted 4E-BP1 is dephosphorylated, induces nuclear translocation of eIF4E, and alters mRNA translation.” Experimental Cell Research: 113246. DOI: 10.1016/j.yexcr.2022.113246 [PubMed: 35697076]

Tang J, Di J, Cao H, Bai J and Zheng J (2015). “p53-mediated autophagic regulation: A prospective strategy for cancer therapy.” Cancer letters 363(2): 101–107. DOI: 10.1016/j.canlet.2015.04.014 [PubMed: 25896632]

Tanida I, Ueno T and Kominami E (2004). “LC3 conjugation system in mammalian autophagy.” The international journal of biochemistry & cell biology 36(12): 2503–2518. DOI: 10.1016/j.biocel.2004.05.009 [PubMed: 15325588]

Tasdemir E, Maiuri MC, Galluzzi L, Vitale I, Djavaheri-Mergny M, D’amelio M, Criollo A, Morselli E, Zhu C and Harper F (2008). “Regulation of autophagy by cytoplasmic p53.” Nature cell biology 10(6): 676–687. DOI: 10.1038/ncb1730 [PubMed: 18454141]

Tooze SA, Dooley HC, Jefferies HB, Joachim J, Judith D, Lamb CA, Razi M and Wirth M (2015). Assessing mammalian autophagy. Membrane Trafficking, Springer: 155–165. DOI: 10.1007/978-1-4939-2309-0_12

Torii S, Yamaguchi H, Nakanishi A, Arakawa S, Honda S, Moriwaki K, Nakano H and Shimizu S (2020). “Identification of a phosphorylation site on Ulk1 required for genotoxic stress-induced alternative autophagy.” Nature communications 11(1): 1–19. DOI: 10.1038/s41467-020-15577-2

Van Nostrand JL, Hellberg K, Luo E-C, Van Nostrand EL, Dayn A, Yu J, Shokhirev MN, Dayn Y, Yeo GW and Shaw RJ (2020). “AMPK regulation of Raptor and TSC2 mediate metformin effects on transcriptional control of anabolism and inflammation.” Genes & development 34(19–20): 1330–1344. DOI: 10.1101/gad.339895.120 [PubMed: 32912901]

Vu TH and Hoffman AR (1997). “Imprinting of the Angelman syndrome gene, UBE3A, is restricted to brain.” Nat Genet 17(1): 12–13. DOI: 10.1038/ng0997-12 [PubMed: 9288087]

Wang P, Li CG, Zhou X and Ding S (2022). “Transcription factor EB enhances autophagy and ameliorates palmitate-induced insulin resistance at least partly via upregulating AMPK activity in skeletal muscle cells.” Clinical and Experimental Pharmacology and Physiology 49(2): 302–310. DOI: 10.1111/1440-1681.13600 [PubMed: 34614219]

Wang T, Wang J, Wang J, Mao L, Tang B, Vanderklish PW, Liao X, Xiong Z-Q and Liao L (2019). “HAP1 is an in vivo UBE3A target that augments autophagy in a mouse model of Angelman syndrome.” Neurobiology of Disease 132: 104585. DOI: 10.1016/j.nbd.2019.104585 [PubMed: 31445164]

Wang W, Xia Z, Farré J-C and Subramani S (2018). “TRIM37 deficiency induces autophagy through deregulating the MTORC1-TFEB axis.” Autophagy 14(9): 1574–1585. DOI: 10.1080/15548627.2018.1463120 [PubMed: 29940807]

Woodcock HV, Eley JD, Guillotin D, Platé M, Nanthakumar CB, Martufi M, Peace S, Joberty G, Poeckel D and Good RB (2019). “The mTORC1/4E-BP1 axis represents a critical signaling node during fibrogenesis.” Nature communications 10(1): 1–16. DOI: 10.1038/s41467-018-07858-8

Yang Y, Zhu Y, Zhou S, Tang P, Xu R, Zhang Y, Wei D, Wen J, Thorne RF and Zhang XD (2022). “TRIM27 cooperates with STK38L to inhibit ULK1-mediated autophagy and promote tumorigenesis.” The EMBO Journal: e109777. DOI: 10.15252/embj.2021109777 [PubMed: 35670107]

Zachari M and Ganley IG (2017). “The mammalian ULK1 complex and autophagy initiation.” Essays in biochemistry 61(6): 585–596. DOI: 10.1042/EBC20170021 [PubMed: 29233870]

Zientara-Rytter K and Subramani S (2019). “The roles of ubiquitin-binding protein shuttles in the degradative fate of ubiquitinated proteins in the ubiquitin-proteasome system and autophagy.” Cells 8(1): 40. DOI: 10.3390/cells8010040 [PubMed: 30634694]

Highlights

- UBE3A deficiency increases autophagy activity in mouse cerebellum and COS-1 cells
- Increased LC3II and decreased p62 indicate enhanced autophagy initiation and flux
- AMPK-ULK1 pathway plays an important role in UBE3A deficiency-induced autophagy
- Reduced cytosolic p53 and enhanced nuclear p53 activation may also play a role

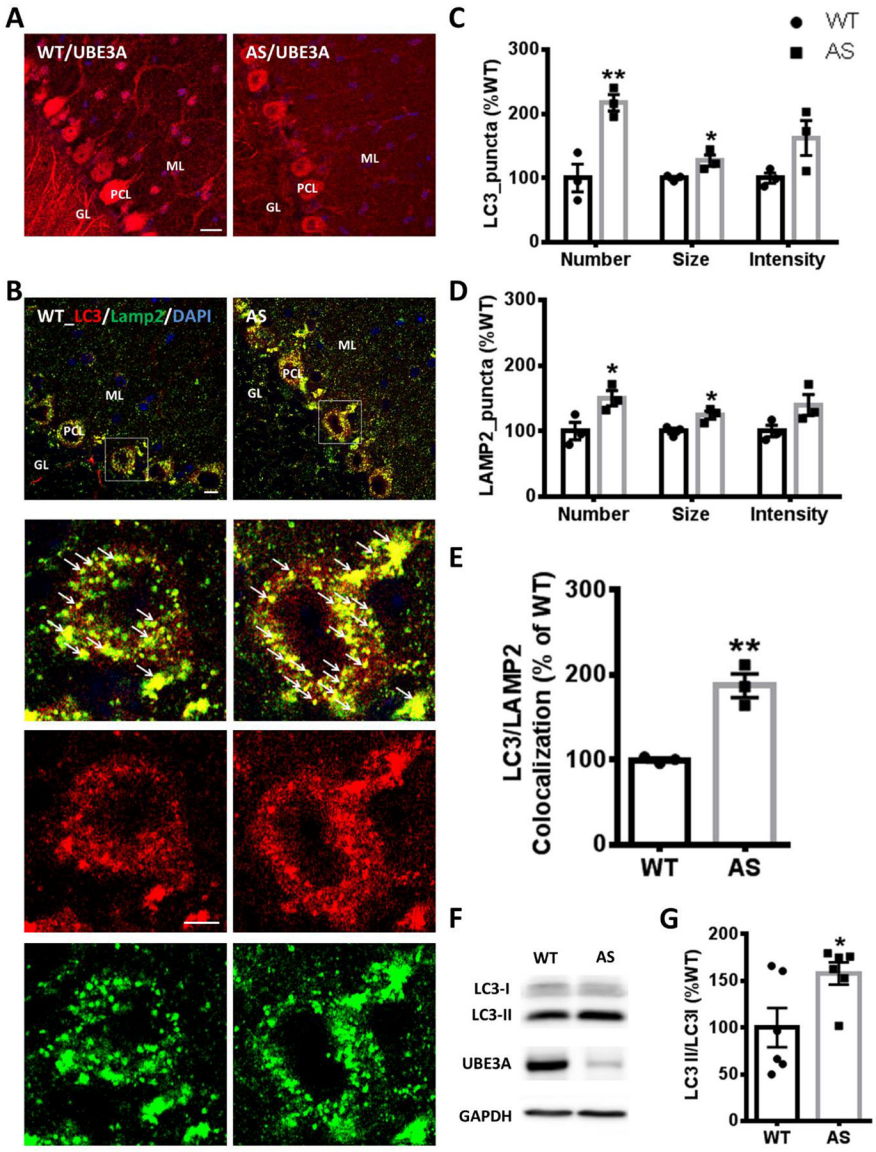

Figure 1.

Characterization of autophagy-lysosome system in the cerebellum of AS mice. ***A***, Expression of UBE3A in the cerebellum of WT and AS mice. Note that UBE3A-ir in Purkinje neurons was significantly reduced in AS mice. Scale bar, 20 μm. ML: molecular layer, PCL: Purkineje cell layer, GL: granular layer. ***B-E***, LC3- and LAMP2-ir puncta were increased in AS cerebellum. Cerebellar sections from AS and WT mice were immunostained with antibodies recognizing the autophagosomes marker LC3 (red) and the lysosomal protein LAMP2 (green). ***B***. Representative images. Bottom panels are enlarged images of LC3 and LAMP2-ir in Purkinje neurons. Arrowheads indicate colocalized puncta. Scale bar: top, 10 μm; bottom, 5 μm. ***C, D***, and ***E***. Quantification of fluorescent signals for LC3 (C), LAMP2 (D), and co-localization of LC3/LAMP2 (E) in WT and AS mice, as shown in ***B*** (means ± SEMs from 3 mice and expressed as % of WT, *p < 0.05, **p < 0.01, Student's t-test). ***F***. Representative images of Western blots of LC3, UBE3A, and GAPDH (used as a

loading control). ***G***. Quantitative analysis of Western blots. Note the significant increase in the ratio of LC3-II/LC3-I in the cerebellum of AS mice as compared to WT mice (mean ± SEM, *$p < 0.05$, $n = 6$, Student's t-test).

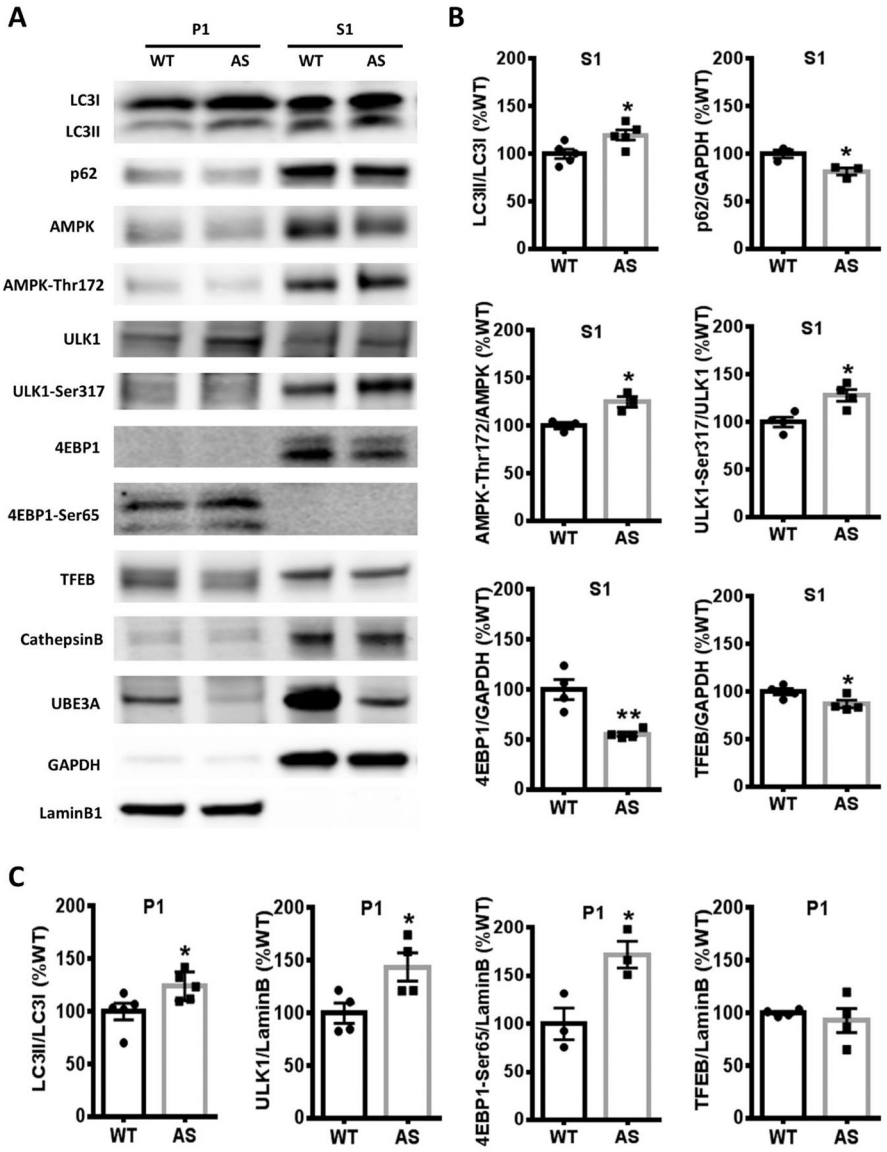

Figure 2.

Levels of autophagic and lysosomal-related proteins were altered in nuclear (P1) and cytoplasmic (S1) fractions in cerebellum of AS mice. ***A*- C**. Western blot analysis of levels of autophagy-lysosome related proteins and of their phosphorylated forms. **A**. Representative images. ***B***. Quantitative data of S1 fraction Western blots shown in ***A*** (means ± SEMs from 3–5 mice, *p < 0.05, **p < 0.01, Student's t-test). ***C***. Quantitative data of P1 fraction Western blots shown in ***A*** (means ± SEMs from 3–5 mice, *p < 0.05, **p < 0.01, Student's t-test).

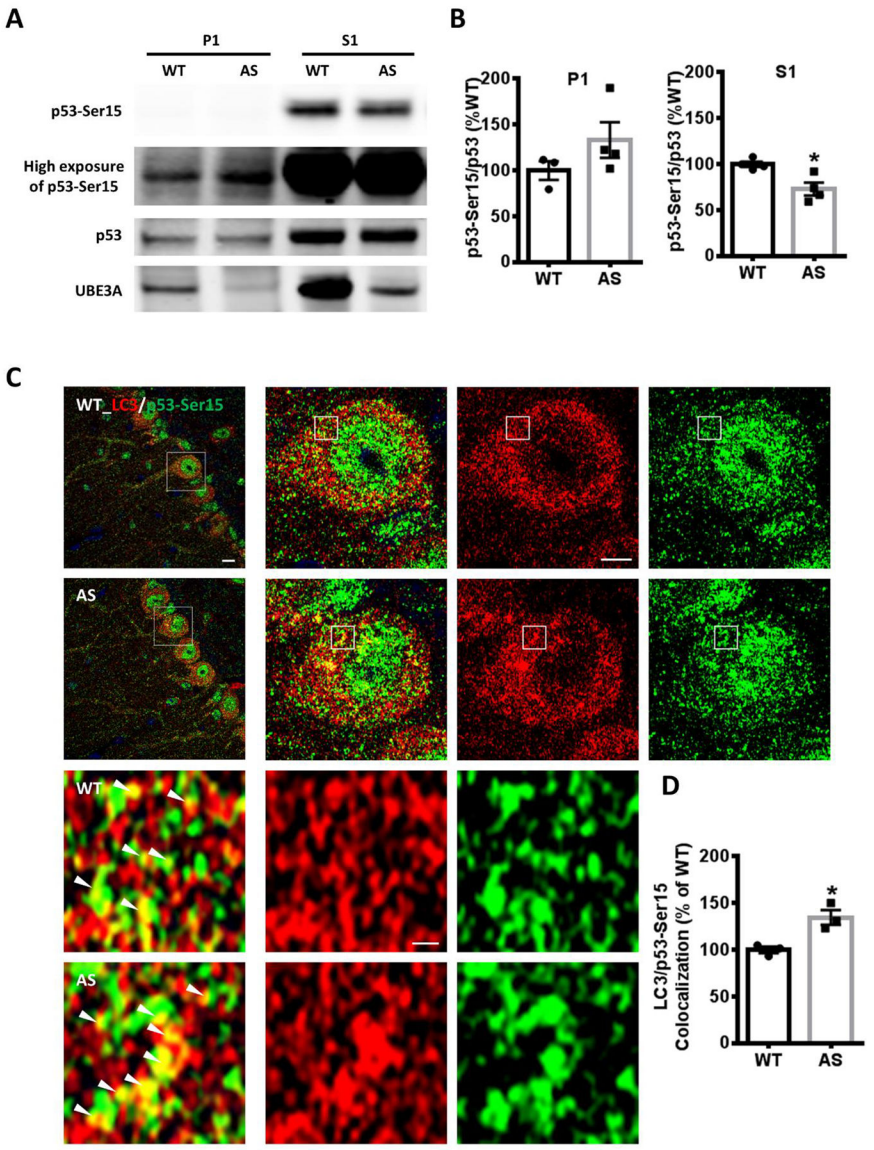

Figure 3.

Expression of p53 and its phosphorylated form, p53-Ser15, in the cerebellum of WT and AS mice. ***A***. Representative images of Western blots labeled with p53-Ser15 and p53 in P1 and S1 fractions. ***B***. Quantitative analysis of Western blots shown in ***A*** (means ± SEMs from 3–4 mice, *p < 0.05, Student's t-test). ***C***. Co-localization of LC3 (red) with p53-Ser15 (green) in Purkinje neurons from WT and AS mice. Bottom panels are enlarged images of LC3 and p53-Ser15 co-immunoreactive puncta in the cell bodies of cerebellar Purkinje neurons. Arrowheads indicate puncta with dual staining. Scale bar: top left, 10 μm; top right, 5 μm; bottom, 0.5 μm. ***D***. Quantification of LC3/p53-Ser15 co-localization in Purkinje neurons from WT and AS mice (means ± SEM expressed as % of WT, n = 3, *p < 0.05, Student's t-test).

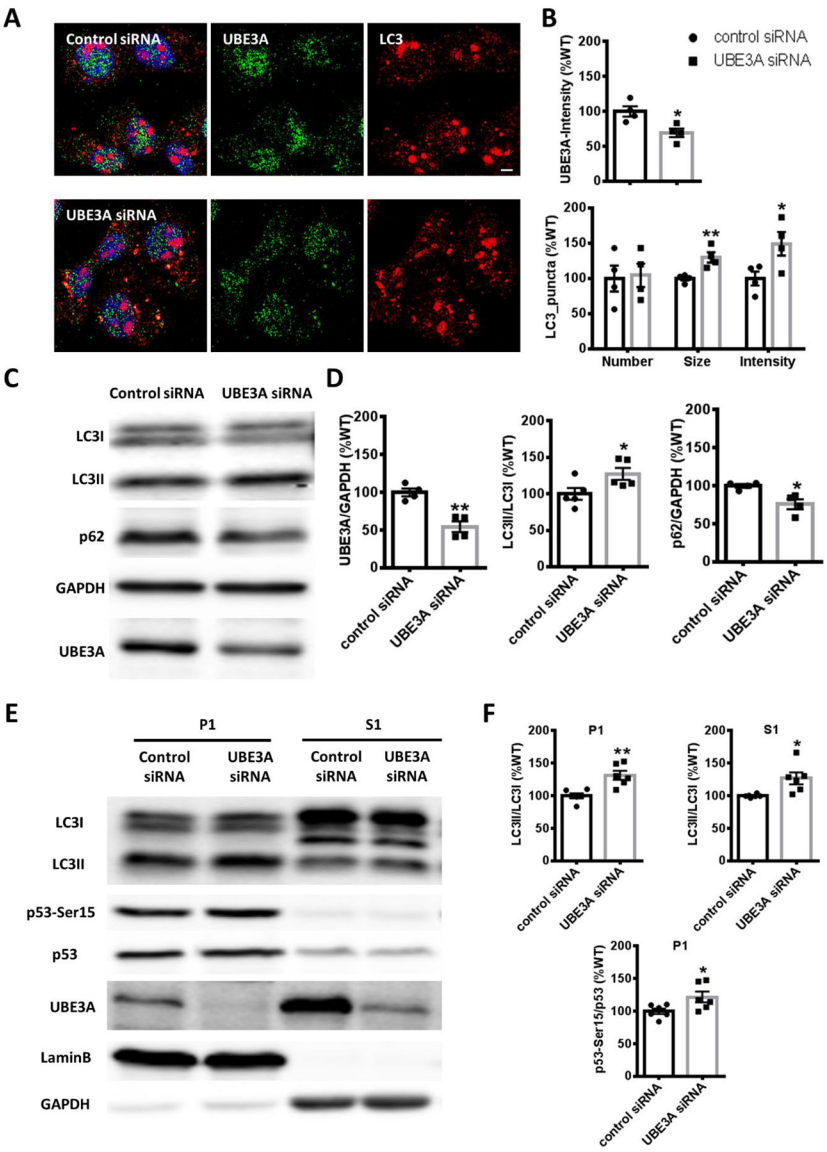

Figure 4.

Knocking down of UBE3A in COS-1 cells increased autophagic induction and flux, which is associated with increased levels of p53-Ser15. ***A***. Expression of LC3 (red puncta) and UBE3A (green) in COS-1 cells transfected with control siRNA and UBE3A siRNA. Scale bar: 5 μm. ***B***. Quantitative analysis of images shown in ***A*** (mean± SEM, n = 4, *p < 0.05, **p < 0.01, Student's t-test). ***C***. Representative images of Western blot processed for LC3, p62, GAPDH, and UBE3A in COS-1 whole homogenates transfected with control siRNA or UBE3A siRNA. ***D***. Western Blot quantitative analysis shown in ***C*** (mean± SEM, n = 4–5, *p < 0.05, **p < 0.01, Student's t-test). ***E***. Representative images of Western blot labeled for LC3, p53, and p53-Ser15 in P1 and S1 fractions from COS-1 cells. ***F***. Quantitative analysis of Western blots shown in ***E*** (mean± SEM, n = 6, *p < 0.05, **p < 0.01, Student's t-test).